

ARTICLES

Reactions of the Dihydroxylamine ($\text{HNO}_2^{\cdot-}$) and Hydronitrite ($\text{NO}_2^{2-\cdot}$) Radical Ions

Sergei V. Lymar,^{*,†} Harold A. Schwarz,[†] and Gidon Czapski[‡]

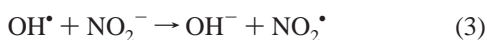
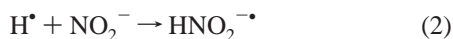
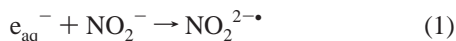
Chemistry Department, Brookhaven National Laboratory, Upton, New York 11973-5000 and Department of Physical Chemistry, The Hebrew University of Jerusalem, Jerusalem 91904, Israel

Received: May 13, 2002

The dihydroxylamine radical anion ($\text{HNO}_2^{\cdot-}$, with the H atom on the nitrogen atom) is produced by the reaction of H atoms in the pulse radiolysis of nitrite solutions and decays in water with a rate constant of $5.0 \times 10^3 \text{ s}^{-1}$. Its absorption spectrum has a maximum at 270 nm with molar absorptivity of $2.8 \times 10^3 \text{ M}^{-1} \text{ cm}^{-1}$. The decay of $\text{HNO}_2^{\cdot-}$ is catalyzed by both acids and bases. The hydronitrite radical ($\text{NO}_2^{2-\cdot}$) produced by the reaction of e_{aq}^- with nitrite exhibits no absorption spectrum between 270 and 550 nm. It is much shorter-lived than $\text{HNO}_2^{\cdot-}$, disappearing at $1.6 \times 10^6 \text{ s}^{-1}$ without generating any $\text{HNO}_2^{\cdot-}$. Neither radical species has any observable $\text{p}K_{\text{a}}$'s, but the $\text{p}K_{\text{a}}$ for $\text{HNO}_2^{\cdot-}$ has been estimated to be lower than 9.3 from the rate data on the hydroxide-catalyzed decomposition of this radical. Both $\text{HNO}_2^{\cdot-}$ and $\text{NO}_2^{2-\cdot}$ reduce methyl viologen, and the reduction by $\text{HNO}_2^{\cdot-}$ has been used to measure its yield, which is found to be 0.63 radicals per 100 eV. Thus, the production of $\text{HNO}_2^{\cdot-}$ by H atoms is quantitative. Collectively, these data represent a major revision of the reductive radiation chemistry of nitrite.

Introduction

The reactions induced by radiation in aqueous nitrite are of considerable importance for environmental chemistry and for radiation chemistry in certain types of nuclear wastes. All three primary radicals from water radiolysis rapidly react with nitrite



The rate constant for the first reaction is $k_1 = 3.5 \times 10^9 \text{ M}^{-1}$

s^{-1} .¹ According to Yost and Russell,² a stable salt of the $\text{NO}_2^{2-\cdot}$ radical has been prepared and is called hydronitrite; the name is derived from a hypothetical hydronitrous acid, $\text{N}(\text{OH})_2^{\cdot}$. An earlier pulse radiolysis study by Grätzel and co-workers³ found UV transient absorption with a maximum at 260 nm, which was assigned to $\text{NO}_2^{2-\cdot}$. From the pH dependence of this absorption, they concluded that the two protic equilibria



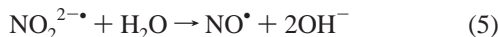
with consecutive $\text{p}K_{\text{a}}$ of 5.7 and 7.7 could be attained within the lifetimes of these radicals. However, these values do not conform to the well-established general rule for oxoacids of the type H_nXO_m , according to which their $\text{p}K_{\text{a}}$ values depend mainly on the $m - n$ difference.⁴ The same rule should apply to radical species^{5,6} and predicts $\text{p}K_{\text{a}} = 8.5 \pm 1$ for $\text{N}(\text{OH})_2^{\cdot}$ and, thus, about 13 for $\text{N}(\text{O})\text{OH}^{\cdot-}$ because the second $\text{p}K_{\text{a}}$ is usually 4–5 units above the first.

* To whom correspondence should be addressed. Phone: (631) 344-4333. Fax: (631) 344-5815. E-mail: lymar@bnl.gov.

[†] Brookhaven National Laboratory.

[‡] The Hebrew University of Jerusalem.

Undoubtedly, the $\text{NO}_2^{2-\bullet}$ radical eventually decays to NO^\bullet , for this is the only stable form of nitrogen(+2), i.e., the reaction



However, the literature on the lifetime of $\text{NO}_2^{2-\bullet}$ is controversial. The half-lives of $12 \mu\text{s}$ ³ and $16 \mu\text{s}$ ⁷ were determined from the decay of transient UV absorption. Other studies that used time-resolved conductivity and photoelectrochemical techniques have found such a long lifetime inconsistent with observations and suggested values $<2 \mu\text{s}$ ⁸ and $0.2 \mu\text{s}$ ⁹ for the $\text{NO}_2^{2-\bullet}$ lifetime.

Grätzel and co-workers³ and, later, Broszkiewicz⁷ assumed that addition of the H atom to NO_2^- in reaction 2 and protonation of $\text{NO}_2^{2-\bullet}$ produced identical species, i.e., that both reactions occurred at an oxygen atom. Using time-resolved EPR, Mezyk and Bartels accurately measured the rate constant for reaction 2, $k_2 = (1.62 \pm 0.05) \times 10^9 \text{ M}^{-1} \text{ s}^{-1}$.¹⁰ They also assumed that the reaction was on an O atom and suggested that the reaction proceeded directly to NO^\bullet and OH^- , without producing $\text{N}(\text{O})\text{OH}^\bullet$ as an intermediate. This conclusion was based largely on ab initio computer modeling, which demonstrated that there was no binding energy for the two products.

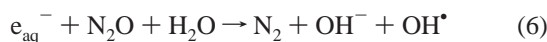
These uncertainties have prompted us to reinvestigate the products of reactions 1 and 2. Here we report that (1) the $\text{NO}_2^{2-\bullet}$ radical decays with a natural lifetime of about $0.6 \mu\text{s}$ and exhibits no absorption spectrum, (2) the species previously observed in UV is the HNO_2^\bullet radical formed by the addition of H^\bullet to the N atom of nitrite, (3) the natural lifetime of this radical is about $200 \mu\text{s}$ and its decomposition is catalyzed by both acids and bases, (4) the $\text{NO}_2^{2-\bullet}$ radical is not a precursor at all for HNO_2^\bullet , and (5) neither protic equilibrium in reaction 4 can be attained and no $\text{p}K_a$ can be observed for any radical species in the system.

Experimental Section

Analytical or ultrapure grade chemicals and Milli-Q purified water were used throughout. The pulse radiolysis was performed with 2 MeV electrons from a van de Graaff accelerator; a 6 cm detection optical path length through a 2 cm cell was used. For the kinetics recorded on a time scale of less than $100 \mu\text{s}$, the analyzing Xe-arc light source was pulsed. Dosimetry was performed with N_2O -saturated 0.01 M KSCN solution using $G\epsilon = 4.87 \times 10^4 \text{ ions (100 eV)}^{-1} \text{ M}^{-1} \text{ cm}^{-1}$ at 472 nm . Pulse widths were in the range $60\text{--}600 \text{ ns}$, which corresponded to doses of up to $1.8 \mu\text{M}$ radicals per unit G value.

Results

Transient Spectra and Products. In qualitative agreement with the previous reports,^{3,7} transient absorption around 270 nm was observed after pulse radiolysis of deaerated nitrite solutions both with and without added *tert*-butyl alcohol (*t*-BuOH). However, nearly the same absorption amplitudes were measured in the presence and absence of N_2O ; a kinetic trace recorded for N_2O -saturated solution is shown in Figure 1. Because N_2O rapidly converts the solvated electron into the OH^\bullet radical



($k_6 = 9.1 \times 10^9 \text{ M}^{-1} \text{ s}^{-1}$),¹¹ this observation rules out the reaction between NO_2^- and e_{aq}^- as the source of the absorbing species.

In these solutions, the OH^\bullet radical was consumed in reaction 3 or in reaction 7

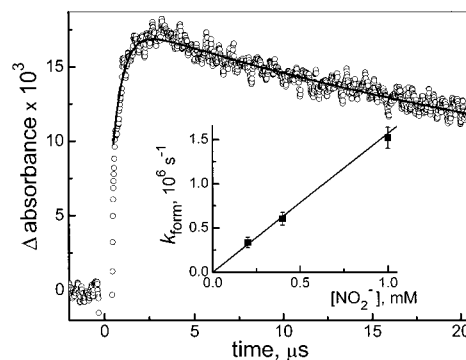
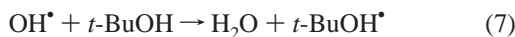


Figure 1. Kinetic trace recorded at 270 nm in N_2O -saturated 1 mM nitrite solution buffered with 4 mM borate, $\text{pH } 9.2$; pulse dose $1.8 \mu\text{M}$ per unit G value. Solid line shows a two-exponential fit with $k_{\text{form}} = 1.6 \times 10^6 \text{ s}^{-1}$ and $k_{\text{decay}} = 3.0 \times 10^4 \text{ s}^{-1}$. Inset: Dependence of k_{form} upon nitrite concentration; line gives a linear fit through origin with a slope of $1.57 \times 10^9 \text{ M}^{-1} \text{ s}^{-1}$.

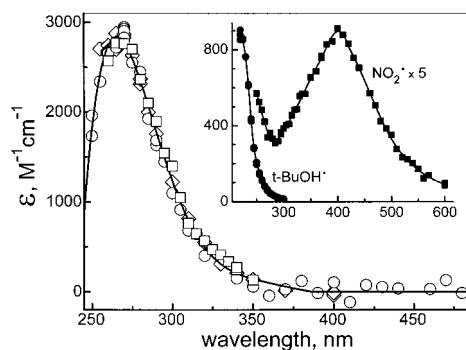


Figure 2. Spectrum of the HNO_2^\bullet radical produced in 1 mM nitrite solution containing 4 mM borate at $\text{pH } 9.2$; pulse dose $1.9 \mu\text{M}$ per unit G value was applied. Other conditions: deaerated (\circ), N_2O -saturated (\square), and deaerated with 0.1 M *t*-BuOH (\diamond) solutions. Inset: Spectrum of the *t*-BuOH $^\bullet$ radical obtained using N_2O -saturated 0.1 M *t*-BuOH solution (\bullet); 5-fold magnified spectrum of the NO_2^\bullet radical obtained in N_2O -saturated 1 mM nitrite solution containing 5 mM NaOH (\blacksquare). Solid lines give smooth representation of data.

Because *t*-BuOH $^\bullet$ and NO_2^\bullet both exhibit appreciable absorption in UV, the observed absorption spectra had to be corrected for these radicals. The *t*-BuOH $^\bullet$ spectrum was redetermined in N_2O -saturated *t*-BuOH solution using $G(t\text{-BuOH}^\bullet) = 6.1$ radicals per 100 eV . Because the fate of the H atoms under these conditions is uncertain, the G value has $\pm 10\%$ accuracy. The obtained spectrum is shown in Figure 2 (inset) and agrees reasonably well with that reported previously.¹² Because the NO_2^\bullet spectrum was not known for wavelengths shorter than 280 nm , it was measured in N_2O -saturated 1 mM nitrite solution containing 5 mM NaOH. As will be shown below, the lifetime of HNO_2^\bullet at this pH is about 100 ns , which is much shorter than the observation time, and so there is no influence of HNO_2^\bullet on the spectrum. The wide-range NO_2^\bullet spectrum calculated using $G(\text{NO}_2^\bullet) = 6.1$ radicals per 100 eV is presented in Figure 2, inset. This spectrum is in a good agreement with the published spectrum³ around 400 nm , but there is a very significant difference in the $280\text{--}350 \text{ nm}$ region which we attribute to the HNO_2^\bullet involvement in the earlier work.

For Ar-saturated 1 mM nitrite solutions with and without *t*-BuOH, practically identical transient spectra with a maximum at 270 nm were obtained after correcting for the *t*-BuOH $^\bullet$ and NO_2^\bullet absorptions (Figure 2). It has been previously assumed³ that these spectra are due to the $\text{NO}_2^{2-\bullet}$ radical, produced in reaction 1. However, the same spectrum was obtained in the

TABLE 1: Rate Constants for Reactions of the $\text{HNO}_2^{\cdot-}$ Radical with Bases and Acids

reactant	rate constant ^a ($\text{M}^{-1} \text{s}^{-1}$)	ionic strength (M)
Bases		
OH^-	1.6×10^9	0.004
NH_3	2.5×10^7	0.01
HPO_4^{2-}	1.5×10^7	0.01
B(OH)_4^-	$< 5 \times 10^6$	0.004
Acids		
H_2O	$5.0 \times 10^3 \text{ s}^{-1}$	0.001
NH_4^+	3.2×10^5	1
H_2PO_4^-	3.1×10^8	0.01
HAc	1.7×10^9	0.002

^a Measured at 25 °C in 1 mM NO_2^- solutions containing 0.1 M *t*-BuOH; all solutions were purged with Ar, except for the buffer-free solution where the saturation with N_2O was used to minimize net production of OH^- ; note the units for H_2O .

presence of N_2O , when corrected for NO_2^{\cdot} absorption (Figure 2). Thus, the spectra in Figure 2 cannot belong to $\text{NO}_2^{2-\cdot}$. Unlike the hydrated electron, the H atoms are rather slowly removed by N_2O (the rate constant of $2.1 \times 10^6 \text{ M}^{-1} \text{ s}^{-1}$ has been reported)¹³ and react preferentially with NO_2^- under these conditions. Therefore, the species absorbing at 270 nm must be the $\text{HNO}_2^{\cdot-}$ radical produced in reaction 2.

This assignment was further confirmed by measuring the dependence upon nitrite concentration of the rate for absorption rise at 270 nm in N_2O -saturated solutions. Kinetic traces such as the one shown in Figure 1 were fit by a sum of two exponentials describing absorbance formation and decay. As shown in Figure 1, inset, the formation rate constant, k_{form} , was linear in $[\text{NO}_2^-]$, from which the second-order rate constant k_2 was found to be $(1.6 \pm 0.1) \times 10^9 \text{ M}^{-1} \text{ s}^{-1}$, in perfect agreement with the value obtained previously¹⁰ from the H atom EPR signal decay in nitrite solutions.

The transient spectra in Figure 2 were determined from similar absorption rise amplitudes, with k_{form} fixed at $1.6 \times 10^6 \text{ s}^{-1}$ for the two-exponential fitting. The apparent $G\epsilon$ values thus obtained were corrected for the contributions from *t*-BuOH $^{\cdot}$ and NO_2^{\cdot} , and the results were divided by $G(\text{H}^{\cdot})$ to compute molar absorptivities. Of the three primary radicals, the H atom yield is the most sensitive to solution composition. That is because it is small, about 20 to 25% of either e_{aq}^- or OH^{\cdot} , and easily affected by solute effects, particularly on the spur H atom production via the $e_{\text{aq}}^- + \text{H}^+$ reaction. The H atom yield used for computing the molar absorptivity of $\text{HNO}_2^{\cdot-}$ in deaerated solution with no added *t*-BuOH was taken as 0.63 radicals per 100 eV, which gave $\epsilon_{270} = 2.8 \times 10^3 \text{ M}^{-1} \text{ cm}^{-1}$. The other two curves in Figure 2 were normalized to this spectrum by adjusting their corresponding $G(\text{H}^{\cdot})$ values. There should be little difference between deaerated nitrite solutions with and without *t*-BuOH; accordingly, the ratio of $G(\text{H}^{\cdot})$ values obtained from normalizing the two was 1.08. The N_2O -saturated solution required $G(\text{H}^{\cdot}) = 0.51$ radicals per 100 eV, which is about 80% of $G(\text{H}^{\cdot})$ for the deaerated solution with no *t*-BuOH.

Reactions of $\text{HNO}_2^{\cdot-}$ with Acids and Bases. The decay of the 270 nm band, which belongs to the $\text{HNO}_2^{\cdot-}$ radical, was accelerated by both acids and bases. These reactions resulted in the complete disappearance of the radical. Neither of the protic equilibria shown in reaction 4 was observed; that is, the rate of $\text{HNO}_2^{\cdot-}$ decay in phosphate buffer, for example, was simply proportional to the concentrations of each H_2PO_4^- and HPO_4^{2-} . The rate constants measured for several acids and bases are summarized in Table 1, which shows that only Brønsted

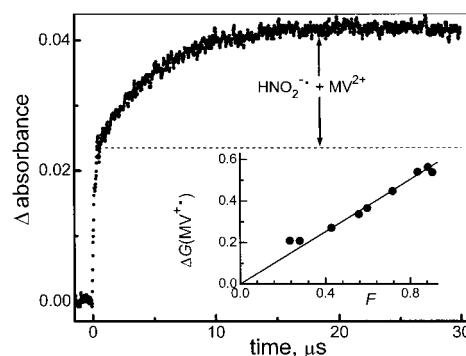
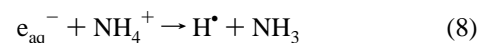


Figure 3. Kinetic trace recorded at 600 nm and showing production of MV^{2+} in deaerated 0.25 mM MV^{2+} solution containing 20 mM NaNO_2 , 0.5 M *t*-BuOH and 0.29 mM phosphate buffer at pH 8.2. The radiation dose was 0.47 μM radicals per unit G value. Inset: Increase in the radiation yield of MV^{2+} (in radicals per 100 eV) due to reaction 9 as a function of the fraction, F , of $\text{HNO}_2^{\cdot-}$ expected to react with MV^{2+} . The slope of the line is 0.63 radicals per 100 eV and gives the total $\text{HNO}_2^{\cdot-}$ radiation yield (eq 11).

acids and bases were efficient decay catalysts. For the ammonium ion, Table 1 gives the value measured in 1 M NH_4Cl . This value is small enough that it may be affected by impurities in the ammonium salt, so that the measured rate constant may represent an upper limit. Notably, the radiation yield observed for $\text{HNO}_2^{\cdot-}$ in this solution was 1.15 radicals per 100 eV, or 0.5 units higher than in the absence of NH_4^+ . This increase is in agreement with reaction 2 being the source of $\text{HNO}_2^{\cdot-}$. Indeed, known rate constants¹¹ predict that about 15 to 20% of e_{aq}^- , or a yield equivalent to about 0.5 radicals per 100 eV, should react with NH_4^+ in Ar-saturated 1 mM NO_2^- solution



and eventually produce additional $\text{HNO}_2^{\cdot-}$.

The reaction rate of $\text{HNO}_2^{\cdot-}$ with water was measured in both buffer-free solution and in solutions containing small amounts of phosphate buffer. In the latter case, the $\text{HNO}_2^{\cdot-}$ decay rate was determined after applying small corrections for the catalysis by HPO_4^{2-} and H_2PO_4^- . Consistent with the net production of OH^- in the buffer-free solutions, the decrease of apparent $\text{HNO}_2^{\cdot-}$ lifetime with increasing radiation dose was observed, and the true lifetime was obtained by extrapolation to zero dose. The decay rate constants determined in these two systems were within 10% of each other and the average was $(5.0 \pm 0.5) \times 10^3 \text{ s}^{-1}$; that is, the natural lifetime of the $\text{HNO}_2^{\cdot-}$ radical in water is about 200 μs . Among the bases, the hydroxyl ion is the most efficient decomposition catalyst; in 5 mM OH^- , the lifetime of $\text{HNO}_2^{\cdot-}$ is reduced to 0.13 μs . This high catalytic efficiency of OH^- allowed measurement of the true NO_2^{\cdot} absorption spectrum shown in Figure 2 (inset), without interference from $\text{HNO}_2^{\cdot-}$. In the previous measurement of the NO_2^{\cdot} spectrum,³ the N_2O -saturated nitrite solution was not made alkaline, hence the persistence of the $\text{HNO}_2^{\cdot-}$ absorption and the mentioned above discrepancy between ours and published spectra at $\lambda < 350 \text{ nm}$.

Reduction of Methyl Viologen (MV^{2+}) by $\text{HNO}_2^{\cdot-}$ and $\text{NO}_2^{2-\cdot}$. These reactions have been followed at 600 nm, where the MV^{2+} radical exhibits strong characteristic absorption with molar absorptivity of $1.4 \times 10^4 \text{ M}^{-1} \text{ cm}^{-1}$ (the average of two reported values^{14,15}). When deaerated solutions containing 0.25 mM MV^{2+} , 20 mM nitrite, and 0.5 M *t*-BuOH were irradiated, the MV^{2+} radical was produced in three distinct stages. The slowest step is shown in Figure 3 and, we suggest it is due to

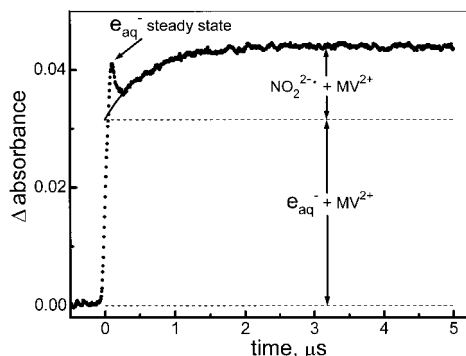


Figure 4. Kinetic trace recorded at 600 nm and showing production of MV^{2+} in deaerated 0.2 mM MV^{2+} solution containing 20 mM $NaNO_2$, 0.5 M *t*-BuOH and 0.01 M NaOH. Radiation dose of 1.23 μM radicals per unit *G* value was applied; pulse width 140 ns. The increase in absorbance above the upper dashed line is the contribution from reaction 12.

the reaction



Its rate was linear in $[MV^{2+}]$, from which the rate constant $k_9 = 6.5 \times 10^8 \text{ M}^{-1} \text{ s}^{-1}$ was determined. Direct reaction of MV^{2+} with the H atom is relatively slow; the rate constant of $6.0 \times 10^8 \text{ M}^{-1} \text{ s}^{-1}$ was reported.¹⁴ Therefore, practically all H atoms reacted with nitrite at the $[NO_2^{\cdot-}]/[MV^{2+}]$ ratio that was used. A small amount of phosphate buffer was added to these solutions, as one of the final reaction products is OH^- generated through reactions 1 and 5. Water and the components of phosphate buffer also react with $HNO_2^{\cdot-}$ (Table 1), so that the fraction of $HNO_2^{\cdot-}$, which can engage in reaction 9, is

$$F = \frac{k_9[MV^{2+}]}{k_9[MV^{2+}] + k_{H_2O} + k_{HPO_4^{2-}}[HPO_4^{2-}] + k_{H_2PO_4^-}[H_2PO_4^-]} \quad (10)$$

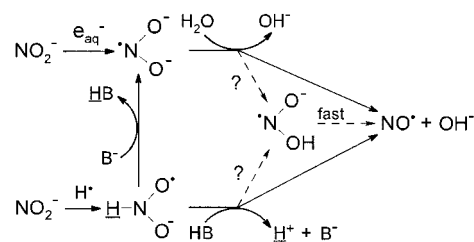
The amplitude of the slow step in Figure 3 should be proportional to *F*; that is, the increase in the radiation yield of $MV^{\cdot+}$ due to this step is expected to be

$$\Delta G(MV^{\cdot+}) = G(HNO_2^{\cdot-}) \times F \quad (11)$$

The value of *F* was modulated by varying concentrations of MV^{2+} , HPO_4^{2-} , and $H_2PO_4^-$. As shown in the inset in Figure 3, a linear relationship between $\Delta G(MV^{\cdot+})$ and *F* was indeed observed. Thus, the species, whose decay is accelerated by phosphate, and the species generating $MV^{\cdot+}$ in the slow step must be the same species. The slope of the $\Delta G(MV^{\cdot+})$ vs *F* dependence gives the yield of $HNO_2^{\cdot-}$, and it is found to be 0.63 ± 0.02 radicals per 100 eV. This value is equal to the yield of H atoms, which indicates that reaction 2 is quantitative and justifies the use of $G(H^{\cdot})$ for computing absorption spectra of $HNO_2^{\cdot-}$ in Figure 2.

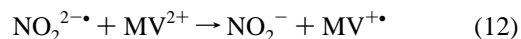
A close examination of the kinetics in Figure 3 reveals two rapid rises at the end of the radiation pulse before the $HNO_2^{\cdot-}$ radical reacts with MV^{2+} . These steps are much more clearly seen in Figure 4, for which the phosphate buffer has been replaced by 0.01 M NaOH. Because OH^- rapidly removed the $HNO_2^{\cdot-}$ radical (Table 1), the slow step due to reaction 9 was 99% eliminated and did not interfere with the measurements of the rapid steps. The fastest rise in Figure 4 is undoubtedly due to a direct reduction of MV^{2+} by e_{aq}^- , for which a rate constant

SCHEME 1



of $7.5 \times 10^{10} \text{ M}^{-1} \text{ s}^{-1}$ has been measured at low ionic strength.¹⁴ The extent of this rise is equivalent to 10% of e_{aq}^- that has been generated and is close to the expected partitioning of e_{aq}^- between MV^{2+} and NO_2^- under the reaction conditions of Figure 4 (0.03 M ionic strength). The hydrated electrons, which absorb very strongly at 600 nm and are present during the radiation pulse in a small steady-state concentration, also contribute to the amplitude of the signal rise and their decay is the cause of the small sharp signal drop at the end of the pulse. The lifetime of e_{aq}^- is about 10 ns in this solution, but the observed lifetime of the drop is actually due more to the decay of the accelerator beam, which occurs over approximately 30 ns.

There is a slower absorbance rise following the e_{aq}^- disappearance in Figure 4. The only species left to explain this step is $NO_2^{2-\cdot}$, i.e., the reaction



The extent of this rise corresponds to about 4% of the total $NO_2^{2-\cdot}$ yield (i.e., the e_{aq}^- yield). This small yield suggests that most of the $NO_2^{2-\cdot}$ have decayed via reaction with water (reaction 5), i.e., $k_{12}[MV^{2+}]/(k_5 + k_{12}[MV^{2+}]) \approx 0.04$. In this case, the rate constant of $1.7 \times 10^6 \text{ s}^{-1}$ observed for the slowest rise step in Figure 4 corresponded to $k_5 + k_{12}[MV^{2+}]$. From these measurements, we derive $k_{12} \approx 3 \times 10^8 \text{ M}^{-1} \text{ s}^{-1}$ and $k_5 \approx 1.6 \times 10^6 \text{ s}^{-1}$, so that the natural lifetime of $NO_2^{2-\cdot}$ in water is about 0.6 μs .

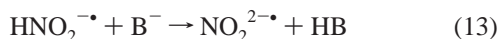
An attempt was made to find an absorption spectrum for the $NO_2^{2-\cdot}$ radical using deaerated 3 mM nitrite solutions also containing 0.1 M *t*-BuOH and 10 mM NaOH. Only the region above 270 nm was available for study, as nitrite itself absorbed too strongly for measurements at shorter wavelengths. The kinetic traces showed the expected presence of *t*-BuOH \cdot radical absorption and vestiges of NO_2^{\cdot} radical immediately after the electron pulse, but no further absorption was seen with a molar absorptivity greater than $50 \text{ M}^{-1} \text{ cm}^{-1}$ anywhere out to 550 nm. Thus, the occurrence of reaction 12 was the only evidence that could be obtained for the presence of $NO_2^{2-\cdot}$ in solution following reaction 1.

Discussion

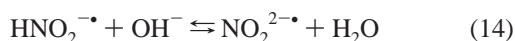
Our observations indicate that H atoms react quantitatively with NO_2^- by addition to the nitrogen atom, whereas acids (including water) always protonate the $NO_2^{2-\cdot}$ radical at its oxygen atom, as shown in Scheme 1. Ab initio calculations¹⁰ found no gas-phase stability for $N(O)OH^{\cdot-}$, and we have observed no evidence for its existence in solution. Thus, it is likely that protonation of $NO_2^{2-\cdot}$ is either simultaneous with or is very rapidly followed by dissociation of $N(O)OH^{\cdot-}$ into $NO^{\cdot} + OH^-$; these alternatives are both shown in Scheme 1. In either case, the NO_2^{\cdot} radical in all its forms persists in aqueous solution for only 0.6 μs , as has been determined from the experiments on MV^{2+} reduction (Figure 4). This value is in

general agreement with a somewhat shorter lifetime of 0.2 μs deduced less directly from photoelectrochemical measurements.⁹

The radical absorbing at 270 nm is $\text{HNO}_2^{\cdot-}$ and not N(O)OH^{\cdot} or $\text{NO}_2^{2-\cdot}$, as has been suggested by Grätzel and co-workers.³ The name “dihydroxylamine radical ion” may be suggested for the $\text{HNO}_2^{\cdot-}$ species, for it can be considered as a product of one-electron oxidation of dihydroxylamine, HN(OH)_2 . The catalysis of the $\text{HNO}_2^{\cdot-}$ decomposition by bases (Table 1) is readily interpreted as the deprotonation reactions followed by rapid decomposition of the $\text{NO}_2^{2-\cdot}$ radical



An upper limit can be estimated for the $\text{p}K_a$ of $\text{HNO}_2^{\cdot-}$, i.e., for the dissociation of nitrogen-bound proton. The forward rate constant for the reaction



is $1.6 \times 10^9 \text{ M}^{-1} \text{ s}^{-1}$ (Table 1). The reverse rate constant is not known, but it must be less than 2% of the total rate of reaction of $\text{NO}_2^{2-\cdot}$ with water (most of which occurs via reaction 5) because the radiation yield of $\text{HNO}_2^{\cdot-}$ is within 10% of the H atom yield, and the $\text{NO}_2^{2-\cdot}$ yield is approximately 5 times the H atom yield. Thus, k_{-14} is less than $3.2 \times 10^4 \text{ s}^{-1}$, and the equilibrium constant $K_{14} = k_{14}/k_{-14} > 5 \times 10^4 \text{ M}^{-1}$, or $\text{p}K_a(\text{HNO}_2^{\cdot-}) < 9.3$. All of the rate constants for bases in Table 1 are in comfortable agreement with this limiting $\text{p}K_a$ estimate. Being a Lewis base, B(OH)_4^- cannot easily accept a proton, hence the immeasurably slow catalysis of the $\text{HNO}_2^{\cdot-}$ decomposition by borate.

The reactions of $\text{HNO}_2^{\cdot-}$ with acids are more difficult to explain. The ostensibly simplest explanation based on acid-catalyzed conversion of $\text{HNO}_2^{\cdot-}$ into N(O)OH^{\cdot} is mechanistically problematic, because the HN(O)OH^{\cdot} radical cannot serve as an intermediate in this conversion. Application of the general $\text{p}K_a$ rule for the oxoacids mentioned in the Introduction section predicts the $\text{p}K_a = 3 \pm 1$ for the dissociation of the oxygen-bound proton in HN(O)OH^{\cdot} . Indeed, the $\text{p}K_a$ of the carbon analogue of HN(O)OH^{\cdot} , formic acid, is 3.75, and the $\text{p}K_a$ of nitrous acid is 3.4. These values are far too low to allow rapid protonation of $\text{HNO}_2^{\cdot-}$ by the acids in Table 1. For example, the equilibrium constant for the reaction



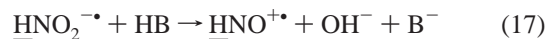
would be 2×10^{-4} , if the $\text{p}K_a$ of HN(O)OH^{\cdot} were 3.5. Because $k_{15} = 3.1 \times 10^8 \text{ M}^{-1} \text{ s}^{-1}$ (Table 1), k_{-15} would have to be $1.6 \times 10^{12} \text{ M}^{-1} \text{ s}^{-1}$, which is impossible. A reasonable diffusion-limited value for k_{-15} is about $3 \times 10^9 \text{ M}^{-1} \text{ s}^{-1}$, which would in turn require $\text{p}K_a$ of 6.2 for HN(O)OH^{\cdot} , in violation of the oxoacid rule. Thus, it would appear that some additional assistance from an internal process in the $\text{HNO}_2^{\cdot-}$ radical is required for the acid-catalyzed decomposition to occur with the observed rates.

Two possible mechanisms for this reaction are shown in Scheme 1. Because by the oxoacid rule, the $\text{p}K_a$ of N(O)OH^{\cdot} must be about 13, i.e., much higher than the estimated above upper limit for $\text{p}K_a$ of $\text{HNO}_2^{\cdot-}$, a rate-limiting displacement protonation could take place, e.g.



This reaction bypasses the energetically unfavorable formation of HN(O)OH^{\cdot} through the expulsion of the underlined proton

occurring simultaneously with the acceptance of another proton from an acid. The rapid dissociation of the N(O)OH^{\cdot} radical to $\text{NO}^{\cdot} + \text{OH}^-$ should then follow. An alternative pathway for the acid-catalyzed process is provided by a heterolytic cleavage of the N–O bond concerted with the acid attack on an oxygen atom of $\text{HNO}_2^{\cdot-}$, i.e., the rate-determining reaction



This reaction is assisted by ejection of the incipient OH^- from the HNO^+ residue. The latter product cannot have any stability and must deprotonate very rapidly. The ability of $\text{HNO}_2^{\cdot-}$ to reduce MV^{2+} , whose reduction potential is -0.45 V ,¹⁶ suggests that the free energy of formation for $\text{HNO}_2^{\cdot-}$ is greater than -2 kcal/mol . This value is sufficiently high for the overall reaction



to be energetically favorable for all the acids in Table 1; even the reaction with H_2O should be exoergic by more than 13 kcal/mol.

By plotting the maximum absorbance amplitudes observed at 270 nm following an electron pulse vs pH in phosphate-buffered solutions, Grätzel and co-workers³ obtained a growing curve with two inflection points at pH 7.7 and 5.7, which they interpreted as the $\text{p}K_a$'s for successive protonations of $\text{NO}_2^{2-\cdot}$. Although the species they were observing was actually $\text{HNO}_2^{\cdot-}$, the question remains as to why they measured any $\text{p}K_a$'s at all for this species. The magnitude of the absorption maximum is kinetically determined by the competing formation and decay reactions of $\text{HNO}_2^{\cdot-}$. Because $\text{HNO}_2^{\cdot-}$ reacts more rapidly with H_2PO_4^- than with HPO_4^{2-} , an inflection point is expected slightly above pH 7.2, which reflects the $\text{p}K_a$ of H_2PO_4^- , not the $\text{p}K_a$ of $\text{HNO}_2^{\cdot-}$ or N(O)OH^{\cdot} . In fact, the pH dependence published by Grätzel and co-workers could be reproduced by calculations using the rate constants from Table 1 in the present work (see Supporting Information for details and graphical comparison). The lower “ $\text{p}K_a$ ” of 5.7 that they have reported is, undoubtedly, due to catalysis of the $\text{HNO}_2^{\cdot-}$ radical decay by the hydrogen ion, which is expected to be much more rapid than catalysis by H_2PO_4^- . In the same work, the half-life of 12 μs for the 270 nm absorbance in an unbuffered solution has been observed, which is in clear disagreement with the natural $\text{HNO}_2^{\cdot-}$ lifetime of 200 μs obtained here. However, the conditions of the previous study, saturation with Ar and pH 9 before irradiation, were not suitable for measuring the $\text{HNO}_2^{\cdot-}$ lifetime. This follows because under these conditions every e_{aq}^- generates an uncompensated OH^- ion via reactions 1 and 5 before the decay of $\text{HNO}_2^{\cdot-}$ begins. Using the data from Table 1, one obtains a 12 μs decay half-time at pH 9.5, which corresponds to radiation dose of about 7 μM per unit G value.

In summary, we have shown that the products obtained from the reduction of nitrite ion by solvated electrons and by hydrogen atoms are not connected through rapid protic equilibrium, as was previously believed. There are several reasons for this mechanistically unusual behavior. First, the H atom quantitatively reacts by addition to the unsaturated N atom of NO_2^- . Presumably, this mode of reactivity is more energetically favorable than the H atom attack on the O atom. Second, the $\text{NO}_2^{2-\cdot}$ radical always protonates at its O atom because, as discussed above, the $\text{p}K_a$ of N(O)OH^{\cdot} should be several units larger than the $\text{p}K_a$ of $\text{HNO}_2^{\cdot-}$. Third, the lifetimes of the $\text{NO}_2^{2-\cdot}$ and N(O)OH^{\cdot} radicals are too short to allow their protic equilibration with $\text{HNO}_2^{\cdot-}$ and HNO(OH)^{\cdot} .

Acknowledgment. This research was carried out at Brookhaven National Laboratory under the auspices of the U.S. Department of Energy under Contract DE-AC02-98CH10886 from the Division of Chemical Sciences, Office of Basic Energy Sciences. We thank Dr. Gábor Merényi for insightful discussions.

Supporting Information Available: Calculation details concerning the pH dependence of maximum absorption amplitude due to the dihydroxylamine radical and graphical comparison with the previously published data (2 pages). This material is available free of charge via the Internet at <http://pubs.acs.org>.

References and Notes

- (1) Elliot, A. J.; McCracken, D. R.; Buxton, G. V.; Wood, N. D. *J. Chem. Soc., Faraday Trans.* **1990**, *86*, 1539.
- (2) Yost, M.; Russell, H., Jr. *Systematic Inorganic Chemistry*; Prentice Hall: New York, 1944; p 58.
- (3) Grätzel, M.; Henglein, A.; Lilie, J.; Beck, G. *Ber. Bunsen-Ges. Phys. Chem.* **1969**, *73*, 646.
- (4) Cotton, F. A.; Wilkinson, G. *Advanced Inorganic Chemistry*, 5th ed.; John Wiley: New York, 1988; p 104.
- (5) Czapski, G.; Lymar, S. V.; Schwarz, H. A. *J. Phys. Chem. A* **1999**, *103*, 3447.
- (6) Lymar, S. V.; Schwarz, H. A.; Czapski, G. *Radiat. Phys. Chem.* **2000**, *59*, 387.
- (7) Broszkiewicz, R. K. *Bull. Acad. Pol. Sci., Ser. Sci. Chim.* **1976**, *24*, 221.
- (8) Barker, G. C.; Fowles, P.; Stringer, B. *Trans. Faraday Soc.* **1970**, *66*, 1509.
- (9) Benderskii, V. A.; Krivenko, A. G.; Ponomarev, E. A. *Sov. Electrochem.* **1989**, *25*, 154.
- (10) Mezyk, S. P.; Bartels, D. M. *J. Phys. Chem. A* **1997**, *101*, 6233.
- (11) Buxton, G. V.; Greenstock, C. L.; Helman, W. P.; Ross, A. B. *J. Phys. Chem. Ref. Data* **1988**, *17*, 513.
- (12) Simic, M.; Neta, P.; Hayon, E. *J. Phys. Chem.* **1969**, *73*, 3794.
- (13) Czapski, G.; Peled, E. *Isr. J. Chem.* **1968**, *6*, 421.
- (14) Solar, S.; Solar, W.; Getoff, N.; Holcman, J.; Sehested, K. *J. Chem. Soc., Faraday Trans. 1* **1982**, *78*, 2467.
- (15) Watanabe, T.; Honda, K. *J. Phys. Chem.* **1982**, *86*, 2617.
- (16) Wardman, P. *J. Phys. Chem. Ref. Data* **1989**, *18*, 1637.